Adaptive Proxy-Based Robust Control Integrated With Nonlinear Disturbance Observer for Pneumatic Muscle Actuators

Yu Cao, *Student Member, IEEE*, Jian Huang, *Senior Member, IEEE*, Cai-Hua Xiong, *Member, IEEE*, Dongrui Wu, *Senior Member, IEEE*, Mengshi Zhang, *Student Member, IEEE*, Zhijun Li, *Senior Member, IEEE*, and Yasuhisa Hasegawa, *Member, IEEE*

***Abstract*—In pneumatic muscle actuators (PMAs)-driven robotic applications, there might exist unpredictable shocks which lead to the sudden change of desired trajectories and large tracking errors. This is dangerous for physical systems. In this article, we propose a novel adaptive proxy-based robust controller (APRC) for PMAs, which is effective in realizing a damped response and regulating the behaviors of the PMA via a virtual proxy. Moreover, the integration of the APRC and the nonlinear disturbance observer further handles the system uncertainties/disturbances and improves the system robustness. According to the Lyapunov theorem, the tracking states of the closed-loop PMA control system are proven to be globally uniformly ultimately bounded through two motion phases. Extensive experiments are conducted to verify the superior performance of our approach, in multiple tracking scenarios.**

***Index Terms*—Adaptive proxy-based robust control, pneumatic muscle actuator, two-phase stability analysis.**

Manuscript received January 5, 2020; revised March 24, 2020; accepted April 29, 2020. Date of publication May 25, 2020; date of current version August 13, 2020. This work was supported in part by the International Science and Technology Cooperation Program of China under Grant 2017YFE0128300, in part by the the Fundamental Research Funds for the Central Universities under Grant HUST: 2019kfyRCPY014, and in part by the Research Fund of PLA of China under Grant BWS17J024. Recommended by Technical Editor Y.-J. Pan and Senior Editor X. Chen. *(Corresponding authors: Jian Huang; Cai-Hua Xiong.)*

Yu Cao, Jian Huang, Dongrui Wu, and Mengshi Zhang are with the Key Laboratory of Image Processing and Intelligent Control, School of Artificial Intelligence and Automation, Huazhong University of Science and Technology, Wuhan 430074, China (e-mail: cao_yu@mail.hust.edu.cn; huang_jan@mail.hust.edu.cn; drwu09@gmail.com; dream_poem@hust.edu.cn).

Cai-Hua Xiong is with the School of Mechanical Science and Engineering and the State Key Laboratory of Digital Manufacturing Equipment and Technology, Huazhong University of Science and Technology, Wuhan 430074, China (e-mail: chxiong@hust.edu.cn).

Zhijun Li is with the Department of Automation, University of Science and Technology, Hefei 230026, China (e-mail: zjli@ieee.org).

Yasuhisa Hasegawa is with the Department of Micro-Nano Systems Engineering, Nagoya University, Nagoya 464-8603, Japan (e-mail: hasegawa@mein.nagoya-u.ac.jp).

This article has supplementary downloadable material available at https://ieeexplore.ieee.org, provided by the authors.

Color versions of one or more of the figures in this article are available online at https://ieeexplore.ieee.org.

Digital Object Identifier 10.1109/TMECH.2020.2997041

I. Introduction

Due to the attractive characteristics, i.e., high power/weight ratio, no mechanical parts, low cost, etc. [1], the pneumatic muscle actuator (PMA) has been widely used in a variety of fields, especially exoskeletons that are effective in power augmentation and rehabilitation training [2]–[4]. Its driving force is converted from the air pressure of the inner bladder, which has the features of nonlinearity, hysteresis, and time-varying parameters [5], making its modeling and control very challenging. Different control strategies have been proposed for the PMA, including proportional-integral-derivative (PID)-based control [6], nonlinear model predictive control [7], [8], sliding-mode control (SMC) [9], fuzzy control [10], adaptive control [11], dynamic surface control [12], etc. Unfortunately, an accurate mathematical model of the PMA is very difficult to obtain in practice, which causes difficulties in precise control. Meanwhile, the traditional PID control, a typical model-free strategy, works in the position control of the PMA. However, some significant issues should be taken into account. First, the high-gain PID controller may cause oscillation and can hardly realize satisfactory performance in the physical PMA applications, due to the slow response of the PMA and limited sampling rate. Second, the PMA is widely used in the field of robot actuation and industry, in which the load, running amplitude, and frequency may change within a certain task. The traditional PID controller with a set of fixed control parameters may not meet the requirements of these applications. Next, from a theoretical viewpoint, it is difficult to theoretically prove the stability of the closed-loop system when no theoretical model is involved. Thus, there is still a strong demand for robust PMA control.

In robotic applications, the idea of using a proxy is common because a proxy enables robots to track the reference with a damped response to unexpected impacts, which results in the improvement of the system security and performance [13]. However, the physical proxy requires a light-weight and compact mechanism that leads to difficulties for designation. The virtual proxy is a remedy to fulfill the requirement of robot control. A typical strategy called proxy-based sliding-mode control (PSMC) [14], which assumes that a zero-quality virtual proxy exists between the controlled object and the desired trajectory, is significantly a model-free strategy. Damme *et al.* [15] presented a PSMC for a two-degree-of-freedom planar manipulator actuated by pleated pneumatic artificial muscles, and such a strategy of position control was developed for piezoelectric-actuated nanopositioning stages in [16]. Another approach supposed that there was a free space around the proxy for the impedance control of a cable-driven system [17]. However, most proxy-based strategies lack stability analysis or depend on a strong conjecture (e.g., see Conjecture 1 in [14]). Therefore, this kind of strategies demands further investigation to establish a sound theoretical foundation.

The robustness of the control strategy is another significant issue for robotic systems. Although the proxy-based strategies have been used in various applications, most of them rarely consider the improvement of system robustness. Nonlinear disturbance observer (NDO)-based control is a common method for improving control performance. The basic idea is to estimate the disturbances/uncertainties from measurable variables before a control action is taken. Consequently, the influence of the disturbances/uncertainties can be suppressed, and the system becomes more robust [18]–[20]. Multiple NDO-based control strategies have been proposed to compensate for the influence of disturbances/uncertainties [21]–[25]. However, to our best knowledge, there are very few researches on the proxy-based control strategy integrated with NDO. This may be due to two challenges. First, most of the proxy-based strategies are model-free control approaches, whereas a typical NDO-based controller requires a mathematical model of the control system. Therefore, the integration of proxy-based strategy and NDO is not straightforward. Second, a more rigorous analysis is needed to guarantee the stability of the system, which should not be based on a strong conjecture.

This article proposes an adaptive proxy-based robust control integrated with nonlinear disturbance observer for the position control of PMAs. Our main contributions are as follows:

1) The proposed adaptive proxy-based robust control extends PSMC from a model-free strategy to a model-based strategy by defining the motion behaviors of the proxy. Accompanied by a nonlinear disturbance observer, the proposed control method retains the original characteristics of smooth and damped motions and greatly improves the robustness of the algorithm.

2) The proposed controller ensures the global stability of the closed-loop system through two stages, in which the controlled object tracks the proxy, and the proxy tracks the reference trajectory, simultaneously. Furthermore, this article elaborately studies the case when the proxy is not zero and finds that the nonzero proxy mass is capable of regulating the behaviors of the controlled object.

3) Real-world experiments are conducted based on a physical PMA platform for validating the effectiveness of the proposed controller, and the results present better tracking accuracy and robustness under various reference trajectories.

Note that a study presents an extended PSMC [26]. Compared with [26], this article proposes a new theoretical proxy-based method by constructing the motion behaviors of the proxy. Integrating with an NDO, this method can strictly guarantee the global stability of the system while improving the robustness and retaining the original characteristics of smooth and damped motions. Meanwhile, this article quantitatively analyzes the effect of proxy on control performance. It turns out that as the proxy mass increases, the system's tracking errors will gradually approach a bound associated with estimation errors of the system's uncertainties/disturbances. To the best of our knowledge, this is the first study to investigate the effect of the virtual proxy on the physical plant.

The rest of this article is organized as follows. Section II introduces the three-element model of the PMA with the lumped disturbances. Section III first proposes the adaptive proxy-based robust controller (APRC) and then extends the APRC to APRC–NDO to improve the system robustness. Section IV presents real-world experiments to demonstrate the effectiveness and robustness of the APRC–NDO. Finally, Section V concludes this article.

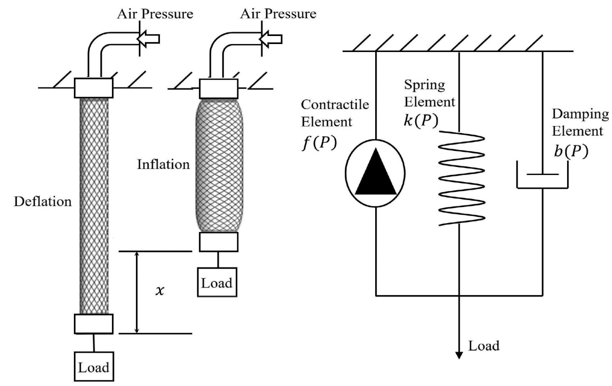

Fig. 1. PMA and its three-element model.

II. Three-Element Model of the PMA

The generalized three-element model of the PMA is shown in Fig. 1 [27]. The contractile length varies with the air pressure of inner bladder. The dynamics of the PMA is

$$\begin{cases} m\ddot{x} + b(P)\dot{x} + k(P)x = f(P) - mg \\ b_i(P) = b_{i0} + b_{i1}P \quad (inflation) \\ b_d(P) = b_{d0} + b_{d1}P \quad (deflation) \\ k(P) = k_0 + k_1 P \\ f(P) = f_0 + f_1 P \end{cases} \tag{1}$$

where m, x, and P are the mass of load, the contractile length of PMA, and the air pressure, respectively. $b(P)$, $f(P)$, and $k(P)$ are the damping coefficient, the contractile force, and the spring coefficient, respectively.

Let $\tau(t)$ denote the sum of unmodeled uncertainties, including unmodeled dynamics, friction, inaccurate parameters, and changing loads. The dynamics of the PMA can be rewritten as a typical second-order nonlinear model

$$\begin{cases} \ddot{x} = f(x,\dot{x}) + b(x,\dot{x})u + \tau(t) \\ f(x,\dot{x}) = \frac{1}{m}(f_0 - mg - b_0\dot{x} - k_0 x) \\ b(x,\dot{x}) = \frac{1}{m}(f_1 - b_1\dot{x} - k_1 x) \end{cases} \tag{2}$$

where u is the air pressure, and $f(x,\dot{x})$ and $b(x,\dot{x})$ are nonlinear terms related to the system states.

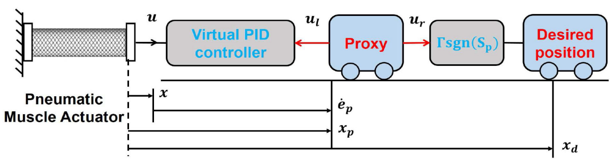

Fig. 2. Principle of proxy-based robust control.

Lemma 1 [28]: Given a differentiable continuous function $\Psi(t)\,\forall t \in [t_0, t_1]$ satisfying $\sigma_1 \le |\Psi(t)| \le \sigma_2$ with positive constant σ_1 and σ_2. The derivative $\dot{\Psi}(t)$ is also bounded.

Assumption 1 [29]: For the system unknown lumped disturbance $\tau(t){:}R^+ \to R$, there exists an unknown positive constant ε such that $\forall t \in R^+$ satisfy $|\tau(t)| < \varepsilon$.

III. Adaptive Proxy-Based Robust Control Integrated With Nonlinear Disturbance Observer

A. Adaptive Proxy-Based Robust Control

The objective of this article is to drive the trajectory of the PMA to track the desired trajectory. In our proxy-based robust controller, an imaginary object called "proxy," assumed to be connected to the physical actuator, is presented. Before introducing the APRC, we define the following sliding manifolds:

$$S_q = \dot{x}_d - \dot{x} + c_1(x_d - x) + c_2\int (x_d - x)\,dt \tag{3}$$

$$S_p = \dot{x}_d - \dot{x}_p + c_1(x_d - x_p) + c_2\int (x_d - x_p)\,dt \tag{4}$$

where c_1 and c_2 are positive constants, x_d the desired trajectory, and x_p and x the proxy position and the PMA's displacement, respectively. First of all, we design a relationship between the proxy and the controlled object to satisfy

$$\dot{S}_q + K_p(x_p - x) + K_i\int (x_p - x)\,dt + K_d(\dot{x}_p - \dot{x}) + \tau = 0 \tag{5}$$

where K_p, K_i, and K_d are positive constants.

Remark 1: Traditionally, once the sliding manifold S_q is defined, the controller can be designed using $\dot{S}_q = -k \cdot \mathrm{sgn}(S_q)$, which is known as the SMC and may cause severe chattering. Hence, our idea of introducing the proxy is to replace $-k \cdot \mathrm{sgn}(S_q)$ by a PID controller to establish a connection between the controlled object and the proxy, as shown in Fig. 2. Note that (5) can also be rewritten as

$$\dot{\mathbf{X}} = \begin{bmatrix} 0 & 1 & 0 \\ 0 & 0 & 1 \\ 0 & -c_2 & -c_1 \end{bmatrix}\mathbf{X} + \begin{bmatrix} 0 \\ 0 \\ 1 \end{bmatrix} u_l + \begin{bmatrix} 0 \\ 0 \\ 1 \end{bmatrix}\rho \tag{6}$$

where $\rho = \ddot{x}_d + c_1\dot{x}_d + c_2 x_d + \tau$, $\mathbf{X} = [\int x dt, x, \dot{x}]^T$, and

$$u_l = K_p(x_p - x) + K_i\int (x_p - x)\,dt + K_d(\dot{x}_p - \dot{x}). \tag{7}$$

It is clear that (6) can be regarded as a local relation between the controlled object and the proxy. This is a linear system with PID control, where $\mathbf{X}$ is the system's states, x_p regarded as the desired trajectory, and $\ddot{x}_d$, $\dot{x}_d$, and x_d are varying parameters unrelated to the system's states. This PID controller drives the PMA's trajectory x to track the proxy's trajectory x_p, when the controller parameters are properly tuned based on the following stability condition.

Hence, bringing (2) and (3) into (5), the control signal fed into the PMA can be computed as follows:

$$u = \frac{1}{b(x,\dot{x})}[\ddot{x}_d + c_1(\dot{x}_d - \dot{x}) + c_2(x_d - x) - f(x,\dot{x}) + K_p(x_p - x) + K_i\int (x_p - x)\,dt + K_d(\dot{x}_p - \dot{x})]. \tag{8}$$

However, x_p is unknown, and x_p should be driven to approach the desired trajectory x_d to fulfill the tracking tasks. A common idea is to use a sign function to ensure the manifold $S_p \to 0$. Hence, we generate the control signal of proxy u_r between the desired trajectory and the proxy, i.e.

$$u_r = \hat{\Gamma} \cdot \mathrm{sgn}(S_p) \tag{9}$$

where $\mathrm{sgn}(S_p)$ is the signum function. $\hat{\Gamma}$ is the adaptive gain of the sliding surface S_p, and the corresponding optimal constant of $\hat{\Gamma}$ is Γ^*.

The adaptive law is described as

$$\dot{\hat{\Gamma}} = \begin{cases} \gamma|S_p|, & |S_p| \ge \delta \\ 0, & |S_p| < \delta \end{cases}, \hat{\Gamma}(0) = 0 \tag{10}$$

where γ is a positive constant that regulates the adaptive rate. δ is a boundary layer. When the system achieves a steady state, $|S_p|$ is small enough, so that $\hat{\Gamma}$ will reach an upper bound instead of monotonically increasing.

Remarkably, the proxy is affected by u_r and u_l, simultaneously, as shown in Fig. 2, and they are not force signals in the traditional sense. Hence, we cannot directly use Newton's law to establish the relationship between the motion behaviors of the proxy and u_r, u_l. Besides, it is necessary to define such property to ensure the realization of tracking and the system's stability. Similar to Newton's law, we define the behavior of the proxy under the effects of u_r and u_l. Let $m_p > 0$ be the so-called proxy mass. Then

$$m_p\dot{S}_p = -u_r + u_l. \tag{11}$$

The effect of $-u_r + u_l$ is similar to the resultant force on the proxy while $m_p\dot{S}_p$ can be seen as the motion principle of the proxy. Note that this property can be arbitrarily defined according to the specific situation, as long as the stability of the closed-loop system can be ensured.

Combining (4), (7), (9), and (11), the trajectory of the proxy is presented as

$$\ddot{x}_p = \frac{1}{m_p}[\hat{\Gamma}\mathrm{sgn}(S_p) - K_p(x_p - x) - K_i\int (x_p - x)\,dt - K_d(\dot{x}_p - \dot{x})] + \ddot{x}_d + c_1(\dot{x}_d - \dot{x}_p) + c_2(x_d - x_p). \tag{12}$$

Once x_p is determined, the control signal of the PMA can then be computed from (4), (8), and (12).

For the convenience of presentation, we first define $\mathbf{K}_m = diag\{K_i c_2, \varpi, K_d\}$ with $\varpi = K_p c_1 - K_i - K_d c_2$.

Theorem 1: The norm of tracking error between the proxy states $\mathbf{X}_p = [\int x_p dt, x_p, \dot{x}_p]^T$ and the system states $\mathbf{X} = [\int x dt, x, \dot{x}]^T$ is uniformly ultimately bounded, and a sliding motion on the surface (4) can be guaranteed when the APRC satisfies

$$m_p > 0, \lambda(\mathbf{K}_c) > 0, \Gamma^* \geq \lambda_2(K_p + K_i + K_d), \varpi > 0$$

where $\lambda(\cdot)$ and $\lambda_{\min}(\cdot)$ denote the eigenvalues and the minimum eigenvalue of the matrix, respectively.

$$\lambda_2 = \frac{(c_1 + c_2 + 1)\varepsilon}{\lambda_{\min}(\mathbf{K}_m)}, \mathbf{K}_c = \begin{bmatrix} K_p c_2 + K_i c_1 & K_i + K_d c_2 \\ K_i + K_d c_2 & K_p + K_d c_1 \end{bmatrix}.$$

Proof: Due to $\lambda(\mathbf{K}_c) > 0$, a Lyapunov candidate is defined as $V = V_1 + V_2 + V_3 > 0$ with

$$V_1 = \frac{1}{2} m_p S_p^2 + \frac{1}{2} S_q^2 \tag{13}$$

$$\begin{aligned} V_2 &= \frac{1}{2} \left[e_p \ \dot{e}_p \right] \mathbf{K}_c \begin{bmatrix} e_p \\ \dot{e}_p \end{bmatrix} \\ &= \frac{1}{2}(K_p + K_d c_1 - K_i - K_d c_2)\dot{e}_p^2 \\ &\quad + \frac{1}{2}(K_p c_2 + K_i c_1 - K_i - K_d c_2) e_p^2 \\ &\quad + \frac{1}{2}(K_i + K_d c_2)(e_p + \dot{e}_p)^2 \end{aligned} \tag{14}$$

$$V_3 = \frac{1}{2\gamma} \tilde{\Gamma}^2 \tag{15}$$

where $e_p = \int (x_p - x) dt$ and $\tilde{\Gamma} = \hat{\Gamma} - \Gamma^*$.

From (7)–(11), it follows that

$$m_p \dot{S}_p = -\hat{\Gamma} \mathrm{sgn}(S_p) + K_p \dot{e}_p + K_i e_p + K_d \ddot{e}_p. \tag{16}$$

According to (3)–(5), we have

$$\dot{S}_q = -K_p \dot{e}_p - K_i e_p - K_d \ddot{e}_p - \tau \tag{17}$$

$$S_p = S_q - (\ddot{e}_p + c_1 \dot{e}_p + c_2 e_p). \tag{18}$$

Integrating (10)–(18), the derivatives of V_1, V_2, and V_3 are

$$\begin{aligned} \dot{V}_1 &= S_p(-\hat{\Gamma} \mathrm{sgn}(S_p) + K_p \dot{e}_p + K_i e_p + K_d \ddot{e}_p) \\ &\quad + S_q(-K_p \dot{e}_p - K_i e_p - K_d \ddot{e}_p - \tau) \qquad (19) \\ &= -\hat{\Gamma}|S_p| - \tau S_q + (K_p \dot{e}_p + K_i e_p + K_d \ddot{e}_p)(S_p - S_q) \\ &= -\hat{\Gamma}|S_p| - \tau S_q - K_d \ddot{e}_p^2 - K_p c_1 \dot{e}_p^2 - K_i c_2 e_p^2 \\ &\quad - (K_p + K_d c_1)\dot{e}_p \ddot{e}_p - (K_i + K_d c_2) e_p \ddot{e}_p \\ &\quad - (K_p c_2 + K_i c_1) e_p \dot{e}_p \end{aligned}$$

$$\begin{aligned} \dot{V}_2 &= (K_p + K_d c_1)\dot{e}_p \ddot{e}_p + (K_p c_2 + K_i c_1) e_p \dot{e}_p \\ &\quad + (K_i + K_d c_2)\dot{e}_p^2 + (K_i + K_d c_2) e_p \ddot{e}_p. \end{aligned} \tag{20}$$

$$\dot{V}_3 = \frac{1}{\gamma} \tilde{\Gamma} \dot{\hat{\Gamma}} = \tilde{\Gamma} |S_p| = \hat{\Gamma} |S_p| - \Gamma^* |S_p|. \tag{21}$$

Then, it follows that

$$\dot{V}_1 + \dot{V}_2 = -\hat{\Gamma}|S_p| - \tau S_q - K_d \ddot{e}_p^2 - \varpi \dot{e}_p^2 - K_i c_2 e_p^2. \tag{22}$$

Note that

$$\Gamma^* \geq \frac{(K_p + K_i + K_d)(1 + c_1 + c_2)}{\min(K_i c_2, \varpi, K_d)} \varepsilon \geq \varepsilon. \tag{23}$$

From (17)–(23), we have

$$\begin{aligned} \dot{V} &= \dot{V}_1 + \dot{V}_2 + \dot{V}_3 \\ &= -\Gamma^* |S_p| - \tau S_q - K_d \ddot{e}_p^2 - \varpi \dot{e}_p^2 - K_i c_2 e_p^2 \\ &\leq -\varepsilon |S_q| + \varepsilon |\ddot{e}_p + c_1 \dot{e}_p + c_2 e_p| \\ &\quad - \tau S_q - K_d \ddot{e}_p^2 - \varpi \dot{e}_p^2 - K_i c_2 e_p^2 \\ &\leq \varepsilon(1 + c_1 + c_2) \|\mathbf{e}_p\| - \lambda_{\min}(\mathbf{K}_m) \|\mathbf{e}_p\|^2 \\ &= - \|\mathbf{e}_p\| \left[\lambda_{\min}(\mathbf{K}_m) \|\mathbf{e}_p\| - \varepsilon(1 + c_1 + c_2)\right] \end{aligned} \tag{24}$$

where $\mathbf{e}_p = \mathbf{X}_p - \mathbf{X} = [e_p, \dot{e}_p, \ddot{e}_p]^T$. It is easy to see that after a sufficiently long time

$$\|\mathbf{e}_p\| \leq \lambda_2. \tag{25}$$

As a result, $\|\mathbf{e}_p\|$ is uniformly ultimately bounded.

Define a new Lyapunov candidate as

$$V_p = \frac{1}{2} m_p S_p^2 + \frac{1}{2\gamma} \tilde{\Gamma}^2. \tag{26}$$

It follows from (16) that

$$\begin{aligned} \dot{V}_p &= m_p S_p \dot{S}_p + \frac{1}{\gamma} \tilde{\Gamma} \dot{\hat{\Gamma}} \\ &= -\Gamma^* |S_p| + (K_p \dot{e}_p + K_i e_p + K_d \ddot{e}_p) S_p \\ &\leq -\Gamma^* |S_p| + \lambda_2(K_p + K_i + K_d) S_p \\ &\leq 0. \end{aligned} \tag{27}$$

When $||\mathbf{e}_p||$ is uniformly ultimately bounded, the achievement of a sliding motion on the surface (4) is guaranteed.

This completes the proof. ■

Remark 2: The stability analysis of the system has two motion phases. First, the norm of the tracking error between the proxy states $\mathbf{X}_p$ and the system states $\mathbf{X}$ is uniformly ultimately bounded. This indicates that the system states converge to the proxy states. Then, the achievement of sliding motion on the surface (4) means that the proxy tracks the reference trajectory, theoretically. In summary, the system states are capable of indirectly tracking the reference, and the stability of the closed-loop system is guaranteed.

Corollary 1: If inequality (25) holds, and initially $x_p = x_d$, then, as the proxy mass m_p increases, S_q will gradually approach a bound associated with the upper bound of the lumped disturbances.

$$\lim_{m_p \to \infty} |S_q| \leq \lambda_2(c_1 + c_2 + 1). \tag{28}$$

Proof: From (16), it follows that

$$|\dot{S}_p| = \frac{1}{m_p} | - \Gamma^* \mathrm{sgn}(S_p) + K_p \dot{e}_p + K_i e_p + K_d \ddot{e}_p|. \tag{29}$$

Since the system is globally uniformly ultimately bounded and a limited Γ^*, we have

$$\lim_{m_p \to \infty} |\dot{S}_p| = 0. \tag{30}$$

The proxy mass m_p is a fixed value in each experiment. Let t_f be the finite duration of the experiment. Then,

$$S_p = \int_0^{t_f} \dot{S}_p dt + \upsilon \tag{31}$$

where υ is the initial value of $x_d - x_p$, which equals zero. Hence, it follows that

$$|S_p| = |\int_0^{t_f} \dot{S}_p dt| \leq \int_0^{t_f} |\dot{S}_p| dt. \tag{32}$$

Combining (30) and (32), we can obtain

$$\lim_{m_p \to \infty} |S_p| = 0. \tag{33}$$

Considering (18) and (25), after a sufficiently long time

$$\begin{aligned} |S_q| &\leq |S_p| + |\ddot{e}_p + c_1 \dot{e}_p + c_2 \ddot{e}_p| \\ &\leq |S_p| + \lambda_2 (c_1 + c_2 + 1). \end{aligned} \tag{34}$$

Finally,

$$\lim_{m_p \to \infty} |S_q| \leq \lambda_2 (c_1 + c_2 + 1). \tag{35}$$

According to the above results, when the proxy mass m_p approaches positive infinity, S_q will approach a bound associated with the the upper bound of the lumped disturbances. This means that m_p can be used to regulate the behaviors of the PMA. Normally, it should be sufficiently large, so that the proxy trajectory will track the reference accurately and realize a damped response.

This completes the proof. ∎

B. Adaptive Proxy-Based Robust Control Integrated With Nonlinear Disturbance Observer

The previous analysis indicates that the APRC can suppress system uncertainties and ensure the uniformly ultimate boundedness of the system states. However, unlike fast-response motors, the response of the PMA system tends to be relatively slow. The excessive gain Γ^* leads to control accuracy degradation and system instability. Therefore, a nonlinear disturbance observer is considered to handle the system uncertainties and increase the system robustness. According to Lemma 1 and Assumption 1, we have

$$|\dot{\tau}| \leq \mu \tag{36}$$

where μ is an unknown constant.

We define an auxiliary variable z to design the nonlinear disturbance observer, as shown

$$\begin{cases} \hat{\tau} = z + \kappa \dot{x} \\ \dot{z} = -\kappa (f(x, \dot{x}) + b(x, \dot{x}) u + \hat{\tau}) \end{cases} \tag{37}$$

where $\hat{\tau}$ is the estimation of disturbances and κ is a constant gain. Therefore, the derivative of $\hat{\tau}$ is

$$\dot{\hat{\tau}} = \dot{z} + \kappa \ddot{x} = \kappa \tilde{\tau} \tag{38}$$

where $\tilde{\tau} = \tau - \hat{\tau}$. Subtracting both sides of (38) from $\dot{\tau}$, we have $\dot{\tilde{\tau}} = \dot{\tau} - \kappa \tilde{\tau}$ with $\dot{\tilde{\tau}} = \dot{\tau} - \dot{\hat{\tau}}$.

Defining a Lyapunov function

$$V_\tau (\tilde{\tau}) = \frac{1}{2} \tilde{\tau}^2 \tag{39}$$

and evaluating $\dot{V}_\tau (\tilde{\tau})$ along (39)

$$\begin{aligned} \dot{V}_\tau (\tilde{\tau}) &= \tilde{\tau} \dot{\tilde{\tau}} = \tilde{\tau} (\dot{\tau} - \kappa \tilde{\tau}) \\ &\leq \mu |\tilde{\tau}| - \kappa \tilde{\tau}^2 \\ &= - |\tilde{\tau}| (\kappa |\tilde{\tau}| - \mu). \end{aligned} \tag{40}$$

Therefore, the estimation error is bounded by

$$|\tilde{\tau}| \leq \tilde{\varepsilon} \tag{41}$$

where $\tilde{\varepsilon} = \mu / \kappa$.

To integrate the nonlinear disturbance observer into the APRC, we only need to redefine (5) as

$$\dot{S}_q + K_p (x_p - x) + K_i \int (x_p - x) \, dt + K_d (\dot{x}_p - \dot{x}) + \tilde{\tau} = 0. \tag{42}$$

Similarly, bringing (2) and (3) into (42), the control signal of the PMA system is

$$u = \frac{1}{b(x, \dot{x})} [\ddot{x}_d + c_1 (\dot{x}_d - \dot{x}) + c_2 (x_d - x) - f(x, \dot{x}) + K_p (x_p - x) + K_i \int (x_p - x) \, dt + K_d (\dot{x}_p - \dot{x}) - \hat{\tau}]. \tag{43}$$

Theorem 2: The norm of $\tilde{\mathbf{e}}_p = [e_p, \dot{e}_p, \ddot{e}_p, \tilde{\tau}]^T$ is uniformly ultimately bounded, and a sliding motion on the surface (4) can be guaranteed when the APRC–NDO satisfies

$$m_p > 0, \lambda(\mathbf{K}_c) > 0, \Gamma^* \geq \lambda_2' (K_p + K_i + K_d), \varpi > 0$$

where $\mathbf{K}_m' = diag\{K_i c_2, \varpi, K_d, \kappa\}$, and

$$\lambda_2' = \frac{\tilde{\varepsilon}(1 + c_1 + c_2) + \mu}{\lambda_{\min}(\mathbf{K}_m')}$$

Proof: We define a new Lyapunov candidate

$$V' = V_1 + V_2 + V_3 + \frac{1}{2} \tilde{\tau}^2 \tag{44}$$

and note that $\Gamma^* \geq \lambda_2' (K_p + K_i + K_d) \geq \tilde{\varepsilon}$.

From (16), (21), (36)–(39), and (42), the derivative of V' is

$$\begin{aligned} \dot{V}' &= -\Gamma^* |S_p| - \tilde{\tau} S_q - K_d \ddot{e}_p^2 - \varpi \dot{e}_p^2 - K_i c_2 e_p^2 + \tilde{\tau} \dot{\tilde{\tau}} \\ &\leq -\tilde{\varepsilon} |S_q| + \tilde{\varepsilon} |\ddot{e}_p + c_1 \dot{e}_p + c_2 e_p| - \tilde{\tau} S_q \\ &\quad - K_d \ddot{e}_p^2 - \varpi \dot{e}_p^2 - K_i c_2 e_p^2 + \mu |\tilde{\tau}| - \kappa \tilde{\tau}^2 \\ &\leq [\tilde{\varepsilon}(1 + c_1 + c_2) + \mu] \|\tilde{\mathbf{e}}_p\| - \lambda_{\min}(\mathbf{K}_m') \|\tilde{\mathbf{e}}_p\|^2 \\ &= - \|\tilde{\mathbf{e}}_p\| (\lambda_{\min}(\mathbf{K}_m') \|\tilde{\mathbf{e}}_p\| - [\tilde{\varepsilon}(1 + c_1 + c_2) + \mu]). \end{aligned} \tag{45}$$

Thus, $\tilde{\mathbf{e}}_p$ is uniformly ultimately bounded by

$$\|\tilde{\mathbf{e}}_p\| \leq \lambda_2'. \tag{46}$$

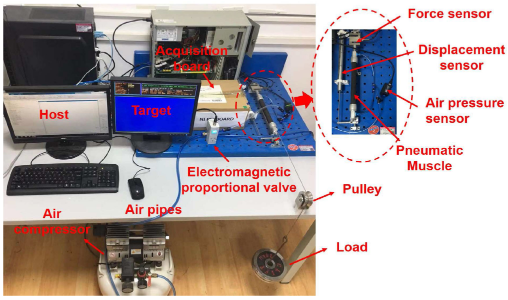

Fig. 3. PMA system.

In this situation, by applying the similar technique in (27), the achievement of a sliding motion on (4) is guaranteed.

$$V_p' = \frac{1}{2} m_p S_p^2 + \frac{1}{2\gamma}\tilde{\Gamma}^2. \tag{47}$$

Thus, the derivative of V_p' is expressed as

$$\begin{aligned}\dot{V}_p' &= m_p S_p \dot{S}_p + \tilde{\Gamma}\dot{\tilde{\Gamma}} \\ &\le -\Gamma^* |S_p| + \lambda_2'(K_p + K_i + K_d) S_p \\ &\le 0.\end{aligned} \tag{48}$$

This completes the proof. ■

Corollary 2: If inequality (46) holds, and initially $x_p = x_d$, then, as the proxy mass m_p increases, S_q will gradually approach a bound associated with estimation errors of the lumped disturbances.

$$\lim_{m_p \to \infty} |S_q| \le \lambda_2'(c_1 + c_2 + 1). \tag{49}$$

Proof: This corollary can be easily proven by using the similar method given in the Proof of Corollary 1. ■

IV. Experiments

A. Experiment Setup

In the physical system, the board (NI-PCI 6052E) enabled A/D and D/A to collect the sensory data and transmitted the control signal to an electromagnetic proportional valve for regulating the inner pressure of the PMA. The air compressor provided compressed air and was connected to the PMA through the electromagnetic proportional valve. Consequently, the displacement of the PMA can be controlled by feedbacking the displacement, as shown in Fig. 3. The PMA was Festo DMSP-20-200N-RM-RM fluidic muscle with an internal diameter of 20 mm, nominal length of 200 mm, and an operating pressure range from 0 to 6 bar. The Festo VPPM-6L-L-1-G18-0L10H-V1P proportional valve was used to regulate the pressure inside the PMA. The displacement sensor was GA-75 whose measurement range was 0–150 mm.

The proposed method does not require an accurate three-element model of the PMA. So, we used the identified parameters of a similar PMA in [11] (see Table I).

We designed two reference trajectories. The first was a fixed frequency sinusoid

$$x_d = A_x \sin(2\pi f_x t) + B_x \tag{50}$$

TABLE I
Model Parameters

Parameter	Value (Unit)	Parameter	Value (Unit)
f_0	−202.32 (N)	f_1	0.00721 (N/Pa)
k_{01}	18063.0 (N/m)	k_{02}	0.01051 (N/(m.Pa))
k_{11}	−0.2132 (N/m)	k_{12}	90638.0 (N/(m.Pa))
b_{0i}	6435.31 (N.s/m)	b_{1i}	0.10023 (N.s/(m.Pa))
b_{0d}	2522.01 (N.s/m)	b_{1d}	0.00321 (N.s/(m.Pa))

where $A_x = 0.015$ m, $f_x = 0.25$ Hz, and $B_x = 0.015$ m. The second was a sine wave whose frequency changed linearly from 0.1 to 0.5 Hz within 20 s. The sampling time was set to 0.001 s.

The maximum absolute error (MAE), the integral of absolute error (IAE), and the relative tracking accuracy (RTE) were used as our performance measurements

$$MAER^a = Max(|x_d(t) - x(t)|_{t=1}^{N}) \tag{51}$$

$$IAER^b = \frac{1}{N}\sum_{t=1}^{N} |x_d(t) - x(t)| \tag{52}$$

$$RTER^c = \frac{\left(\sum_{t=1}^{N} |x_d(t) - x(t)|\right)/N}{x_a} \times 100\% \tag{53}$$

where N is the total sampling time. x_a is the maximum running displacement of the PMA.

The following set of control parameters of the APRC–NDO was used in all experiments: $c_1 = 177.4$, $c_2 = 174.4$, $K_p = 2473.5$, $K_i = 1916$, $K_d = 194.2$, $\kappa = 15952$, $\gamma = 10$. Note that the parameter selections of all the control strategies were based on an optimization algorithm, called switch-mode firefly algorithm (SMFA). More related details can be found in [30].

B. Experimental Results

Fig. 4 shows the experimental results that verified Corollary 1. In this experiment, we selected a fixed Γ^* to demonstrate the influence of $m_p = \{0.5, 1.0, 5.0, 10.0, 15.0\}$. As m_p increased, the tracking accuracy improved, and the variation of S_q significantly decreased. Meanwhile, x_p tracked the reference trajectory more accurately and $|S_p| \to 0$.

Then, we intended to verify the experimental results of the proposed control strategy with different amplitudes of the desired trajectories, as shown in Fig. 5. The corresponding control performances were similar, and the control parameters did not change for this experiment, which indicated that the proposed method is applicable to various applications.

Next, for a fair comparison, the control parameters for all the strategies [APRC–NDO, NDO–SMC, supertwisting algorithm (STA), PSMC] were adjusted with the fixed-frequency sinusoidal reference ($f_x = 0.25$ Hz, $A_x = 0.015$ m, $B_x = 0.015$ m) by the SMFA. Fig. 6 shows the corresponding performance of different control strategies, and the corresponding MAEs, IAEs, and RTEs of all five control strategies are shown in Table II. We replaced the *sign* function of the NDO–SMC with a *sat* function to eliminate chattering. In spite of the inaccurate model parameters in Table I, the NDO–SMC and STA were capable of handling the uncertainties and achieving favorable performance. Meanwhile, the basic PSMC enabled the PMA to track the

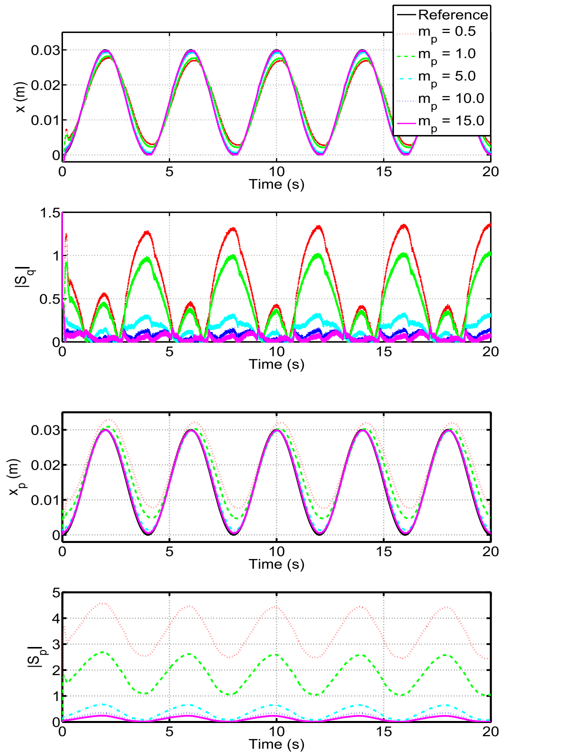

Fig. 4. Tracking performance of the APRC–NDO with different m_p values.

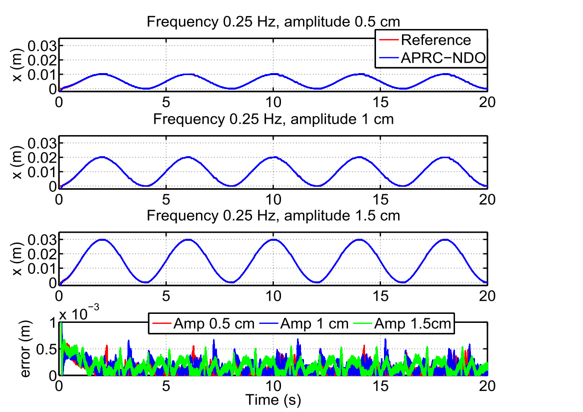

Fig. 5. Tracking performance of the APRC–NDO with different amplitudes of the desired trajectories.

reference with acceptable precision, since it is a model-free strategy, not affected by inaccurate model parameters. However, its performance was still unsatisfied than APRC–NDO. Besides, according to our previous study [8], although the traditional PID controller tracked the reference trajectory, the performance was worse than the proposed strategy. On the other hand, because we had $|S_p| \to 0$, the adaptive coefficient $\hat{\Gamma}$ gradually tended to be a fixed value, instead of monotonically increasing.

Based on the previous tuned control parameters, Fig. 7 showed the tracking performance of different control strategies with the varying-frequency (0.1–0.5 Hz) sinusoidal reference. Although the NDO–SMC behaved well in the steady state, it had a large oscillation at the beginning. On the contrary, the STA performed well at the beginning, but it could not effectively track the reference as the frequency increased. Still, the PSMC tracked the reference with acceptable precision. The proposed APRC–NDO performed the best among all four control strategies, although it had a relatively little oscillation at the beginning. This was because the APRC–NDO needed some time to drive the states of the PMA into the boundary [see (25) and (46)]. After that, the proposed APRC–NDO could handle the system disturbances/uncertainties and achieve accurate tracking. Actually, the NDO is very important, because the uncertainties/disturbances of the system relate to the frequency of PMA's trajectory, and

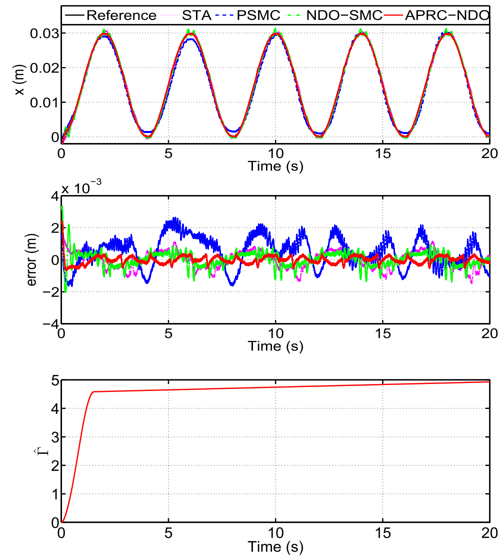

Fig. 6. Tracking performance of different control strategies with the fixed-frequency sinusoidal reference (0.25 Hz).

TABLE II
TRACKING PERFORMANCE OF DIFFERENT CONTROL STRATEGIES WITH THE FIXED-FREQUENCY SINUSOIDAL REFERENCE (0.25 Hz)

	MAE	IAE	RTE
APRC-NDO	5.5×10^{-4} (m)	1.6×10^{-4} (m)	0.5%
PSMC	2.7×10^{-3} (m)	8.9×10^{-4} (m)	2.9%
NDO-SMC	1.4×10^{-3} (m)	3.5×10^{-4} (m)	1.2%
STA	1.5×10^{-3} (m)	4.5×10^{-4} (m)	1.5%
PID [8]	4.0×10^{-3} (m)	1.5×10^{-3} (m)	6.0%

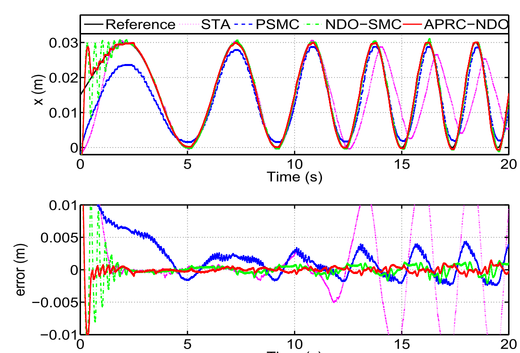

Fig. 7. Tracking performance of different control strategies with the varying-frequency sinusoidal reference (0.1–0.5 Hz).

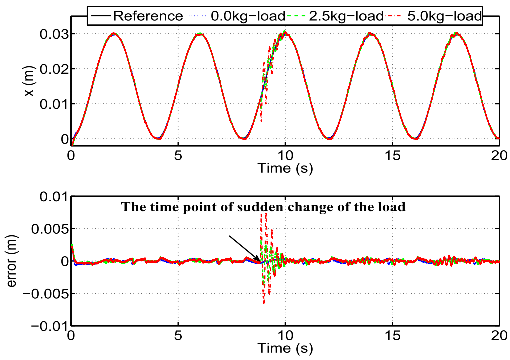

Fig. 8. Tracking performance of the APRC–NDO with a sudden change of load.

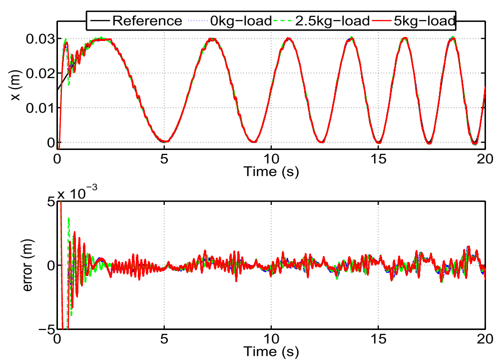

Fig. 9. Tracking performance of the APRC–NDO with the PMA attaching different loads.

the varying frequency causes the growth of the system's uncertainties/disturbances. The SMC and APRC integrated with NDO can better handle the uncertainties/disturbances of the system.

To further investigate the robustness of the proposed control strategy, we first designed an experiment, in which a sudden change of the load (2.5-kg load or 5.0-kg load) was added to the PMA during operation, as shown in Fig. 8. It is seen that the trajectory of the PMA deviated significantly from the reference, and the greater the sudden disturbance, the further it deviated. Moreover, additional experiments were conducted for tracking the varying-frequency (0.1–0.5 Hz) reference with different loads, as shown in Fig. 9. Generally, they were very robust to the changing loads. However, the fixed parameters of the NDO can only handle a certain amount of disturbances. When the disturbance is beyond a certain degree, the parameters of NDO have to be retuned.

V. Conclusion

This article presented a robust control strategy, APRC–NDO, for the PMA. The APRC–NDO can realize a damped response and regulate the behaviors of the PMA via a virtual proxy, as well as handle the system uncertainties/disturbances to improve the robustness. The tracking states of the PMA were proven to be uniformly ultimately bounded through two motion phases. Finally, extensive experiments demonstrated the superior performance of the APRC–NDO.

References

[1] M. A. M. Dzahir and S.-I. Yamamoto, "Recent trends in lower-limb robotic rehabilitation orthosis: Control scheme and strategy for pneumatic muscle actuated gait trainers," *Robotics*, vol. 3, no. 2, pp. 120–148, Mar. 2014.

[2] J. Cao, S. Q. Xie, and R. Das, "MIMO sliding mode controller for gait exoskeleton driven by pneumatic muscles," *IEEE Trans. Control Syst. Technol.*, vol. 26, no. 1, pp. 274–281, Jan. 2018.

[3] Z. Li, B. Huang, A. Ajoudani, C. Yang, C. Su, and A. Bicchi, "Asymmetric bimanual control of dual-arm exoskeletons for human-cooperative manipulations," *IEEE Trans. Robot.*, vol. 34, no. 1, pp. 264–271, Feb. 2018.

[4] Z. Li, B. Huang, Z. Ye, M. Deng, and C. Yang, "Physical human–robot interaction of a robotic exoskeleton by admittance control," *IEEE Trans. Ind. Electron.*, vol. 65, no. 12, pp. 9614–9624, Dec. 2018.

[5] D. G. Caldwell, G. A. Medrano-Cerda, and M. Goodwin, "Control of pneumatic muscle actuators," *IEEE Control Syst.*, vol. 15, no. 1, pp. 40–48, Feb. 1995.

[6] G. Andrikopoulos, G. Nikolakopoulos, and S. Manesis, "Advanced nonlinear PID-based antagonistic control for pneumatic muscle actuators," *IEEE Trans. Ind. Electron.*, vol. 61, no. 12, pp. 6926–6937, Dec. 2014.

[7] J. Huang, J. Qian, L. Liu, Y. Wang, C. Xiong, and S. Ri, "Echo state network based predictive control with particle swarm optimization for pneumatic muscle actuator," *J. Franklin Inst.*, vol. 353, no. 12, pp. 2761–2782, 2016.

[8] J. Huang, Y. Cao, C. Xiong, and H. Zhang, "An echo state Gaussian process-based nonlinear model predictive control for pneumatic muscle actuators," *IEEE Trans. Autom. Sci. Eng.*, vol. 16, no. 3, pp. 1071–1084, Jul. 2019.

[9] J. H. Lilly and L. Yang, "Sliding mode tracking for pneumatic muscle actuators in opposing pair configuration," *IEEE Trans. Control Syst. Technol.*, vol. 13, no. 4, pp. 550–558, Jul. 2005.

[10] S.Q. Xie and P.K. Jamwal, "An iterative fuzzy controller for pneumatic muscle driven rehabilitation robot," *Expert Syst. Appl.*, vol. 38, no. 7, pp. 8128–8137, Jul. 2011.

[11] L. Zhu, X. Shi, Z. Chen, H. Zhang, and C. Xiong, "Adaptive servomechanism of pneumatic muscle actuators with uncertainties," *IEEE Trans. Ind. Electron.*, vol. 64, no. 4, pp. 3329–3337, Apr. 2017.

[12] J. Wu, J. Huang, Y. Wang, and K. Xing, "Nonlinear disturbance observer-based dynamic surface control for trajectory tracking of pneumatic muscle system," *IEEE Trans. Control Syst. Technol.*, vol. 22, no. 2, pp. 440–455, Mar. 2014.

[13] X. Li, Y. Pan, G. Chen, and H. Yu, "Adaptive human–robot interaction control for robots driven by series elastic actuators," *IEEE Trans. Robot.*, vol. 33, no. 1, pp. 169–182, Feb. 2017.

[14] R. Kikuuwe, S. Yasukouchi, H. Fujimoto, and M. Yamamoto, "Proxy-based sliding mode control: A safer extension of PID position control," *IEEE Trans. Robot.*, vol. 26, no. 4, pp. 670–683, Aug. 2010.

[15] M. V. Damme, B. Vanderborght, B. Verrelst, R. V. Ham, F. Daerden, and D. Lefeber, "Proxy-based sliding mode control of a planar pneumatic manipulator," *Int. J. Robot. Res.*, vol. 28, no. 2, pp. 266–284, Feb. 2009.

[16] G. Gu, L. Zhu, C. Su, H. Ding, and S. Fatikow, "Proxy-based sliding-mode tracking control of piezoelectric-actuated nanopositioning stages," *IEEE/ASME Trans. Mechatron.*, vol. 20, no. 4, pp. 1956–1965, Aug. 2015.

[17] K. Kong, "Proxy-based impedance control of a cable-driven assistive system," *Mechatronics*, vol. 23, no. 1, pp. 147–153, Feb. 2013.

[18] Y. Yan, J. Yang, Z. Sun, C. Zhang, S. Li, and H. Yu, "Robust speed regulation for PMSM servo system with multiple sources of disturbances via an augmented disturbance observer," *IEEE/ASME Trans. Mechatron.*, vol. 23, no. 2, pp. 769–780, Apr. 2018.

[19] J. Han, "From PID to active disturbance rejection control," *IEEE Trans. Ind. Electron.*, vol. 56, no. 3, pp. 900–906, Mar. 2009.

[20] D. X. Ba, T. Q. Dinh, J. Bae, and K. K. Ahn, "An effective disturbance-observer-based nonlinear controller for a pump-controlled hydraulic system," *IEEE/ASME Trans. Mechatron.*, vol. 25, no. 1, pp. 32–43, Feb. 2020.

[21] J. Huang, S. Ri, T. Fukuda, and Y. Wang, "A disturbance observer based sliding mode control for a class of underactuated robotic system with mismatched uncertainties," *IEEE Trans. Autom. Control*, vol. 64, no. 6, pp. 2480–2487, Jun. 2019.

[22] J. Huang, M. Zhang, S. Ri, C. Xiong, Z. Li, and Y. Kang, "High-order disturbance-observer-based sliding mode control for mobile wheeled inverted pendulum systems," *IEEE Trans. Ind. Electron.*, vol. 67, no. 3, pp. 2030–2041, Mar. 2020.

[23] Z. Li, J. Li, S. Zhao, Y. Yuan, Y. Kang, and C. L. P. Chen, "Adaptive neural control of a kinematically redundant exoskeleton robot using brain–machine interfaces," *IEEE Trans. Neural Netw. Learn. Syst.*, vol. 30, no. 12, pp. 3558–3571, Dec. 2019.

[24] W. He, Z. Yan, C. Sun, and Y. Chen, "Adaptive neural network control of a flapping wing micro aerial vehicle with disturbance observer," *IEEE Trans. Cybern.*, vol. 47, no. 10, pp. 3452–3465, Oct. 2017.

[25] M. Chen, S. Y. Shao, and B. Jiang, "Adaptive neural control of uncertain nonlinear systems using disturbance observer," *IEEE Trans. Cybern.*, vol. 47, no. 10, pp. 3110–3123, Oct. 2017.

[26] W. Zhao, A. Song, and Y. Cao, "An extended proxy-based sliding mode control of pneumatic muscle actuators," *Appl. Sci.*, vol. 9, no. 8, p. 1571, Apr. 2019.

[27] D. B. Reynolds, D. W. Repperger, C. A. Phillips, and G. Bandry, "Modeling the dynamic characteristics of pneumatic muscle," *Ann. Biomed. Eng.*, vol. 31, pp. 310–317, Mar. 2003.

[28] L. Zhang, Z. Li, and C. Yang, "Adaptive neural network based variable stiffness control of uncertain robotic systems using disturbance observer," *IEEE Trans. Ind. Electron.*, vol. 64, no. 3, pp. 2236–2245, Mar. 2017.

[29] T. P. Zhang and S. S. Ge, "Adaptive dynamic surface control of nonlinear systems with unknown dead zone in pure feedback form," *Automatica*, vol. 44, no. 7, pp. 1895–1903, Jul. 2008.

[30] Y. Cao, J. Huang, Z. Huang, X. Tu, and S. Mohammed, "Optimizing control of passive gait training exoskeleton driven by pneumatic muscles using switch-mode firefly algorithm," *Robotica*, vol. 37, no. 12, pp. 2087–2103, Dec. 2019.

Yu Cao (Student Member, IEEE) received the B.S. degree in control science and control engineering from the Wuhan University of Technology, Wuhan, China, in 2011, and the M.S degree in software engineering from the Huazhong University of Science and Technology, Wuhan, China, in 2014. He is currently working toward the Ph.D. degree in control science and engineering with the Huazhong University of Science and Technology.

His current research interests include nonlinear system control, modeling and control of pneumatic muscle actuators, soft robotics, rehabilitation robotics exoskeleton systems.

Jian Huang (Senior Member, IEEE) graduated from the Huazhong University of Science and Technology (HUST), Wuhan, China, in 1997 and received the Master of Engineering degree and the Ph.D. degree in control science and engineering from HUST in 2000 and 2005, respectively.

From 2006 to 2008, he was a Postdoctoral Researcher at the Department of Micro-Nano System Engineering and the Department of Mechano-Informatics and Systems, Nagoya University, Japan. He is currently a Full Professor with the School of Artificial Intelligence and Automation, HUST. His main research interests include rehabilitation robot, robotic assembly, networked control systems and bioinformatics.

Cai-Hua Xiong (Member, IEEE) received the Ph.D. degree in mechanical engineering from the Huazhong University of Science and Technology (HUST), Wuhan, China, in 1998.

From 1999 to 2003, he was a Postdoctoral Fellow with the City University of Hong Kong, Hong Kong, and The Chinese University of Hong Kong, Hong Kong, and a Research Scientist with the Worcester Polytechnic Institute, Worcester, MA, USA. He is currently a Chang Jiang Professor and the Director of the Institute of Rehabilitation and Medical Robotics, HUST. His current research interests include biomechatronic prostheses, rehabilitation robotics, and robot motion planning and control. Dr. Xiong received the National Science Fund for Distinguished Young Scholars of China.

Dongrui Wu (Senior Member, IEEE) received the Ph.D. degree in electrical engineering from the University of Southern California, Los Angeles, CA, USA, in 2009.

He was a Lead Researcher with GE Global Research and the Chief Scientist of several startups. He is currently a Professor with the School of Artificial Intelligence and Automation, Huazhong University of Science and Technology, Wuhan, China. He has authored or coauthored more than 100 publications, including a book entitled Perceptual Computing (New York, NY, USA: Wiley-IEEE Press, 2010). His research interests include affective computing, brain-computer interface, computational intelligence, and machinelearning.

Prof. Wu was a Recipient of the IEEE Computational Intelligence Society Outstanding Ph.D. Dissertation Award in 2012, the IEEE Transactions on Fuzzy Systems Outstanding Paper Award in 2014, the NAFIPS Early Career Award in 2014, and the IEEE Systems, Man, and Cybernetics Society Early Career Award in 2017. He is an Associate Editor for the IEEE Transactions on Fuzzy Systems, the IEEE Transactions on Human-Machine Systems, and the IEEE Computational Intelligence Magazine.

Mengshi Zhang (Student Member, IEEE) was born in Hubei Province, China, in 1995. She received the B.S. degree in automation from the South-Central University for Nationalities, Wuhan, China, in 2017. She is currently working toward the Ph.D. degree in control science and engineering with the Huazhong University of Science and Technology.

Her current research interests include modeling and control of mobile robot and underactuated systems.

Zhijun Li (Senior Member, IEEE) received the Ph.D. degree in mechatronics from the Shanghai Jiao Tong University, P. R. China, in 2002. From 2003 to 2005, he was a Postdoctoral Fellow in Department of Mechanical Engineering and Intelligent systems, The University of Electro-Communications, Tokyo, Japan.

From 2005 to 2006, he was a Research Fellow in the Department of Electrical and Computer Engineering, National University of Singapore, and Nanyang Technological University, Singapore. Since 2012, he was a Professor in College of Automation Science and Engineering, South China university of Technology, Guangzhou, China. From 2017, he is a Professor in Department of Automation, University of Science and Technology, Hefei, China. From 2016, he has been the Co-Chairs of IEEE SMC Technical Committee on Bio-mechatronics and Bio-robotics Systems (B2S), and IEEE-RAS Technical Committee on Neuro-Robotics Systems.

Dr. Li is serving as an Editor-at-Large of Journal of Intelligent & Robotic Systems.

Yasuhisa Hasegawa (Member, IEEE) received the B.E., M.E., and Ph.D. degrees from Nagoya University, Nagoya, Japan, in 1994, 1996, and 2001, respectively.

In 2003, he was an Assistant Professor at Gifu University, Japan. He moved to the University of Tsukuba in 2004 and became an Associate Professor in 2007. Since 2014, he has been a Professor with Nagoya University. He is leading the Intelligent Robotics Laboratory, Micro-Nano Mechanical Science and Engineering, Nagoya University. His research interests include fundamental and applied studies of mechatronics technologies for advanced human assistive systems.

Dr. Hasegawa is also AdCom Member of RAS, IEEE and the Deputy Chief Editor of the Journal of Robotics and Mechatronics.